

# Environmentally compatible and highly improved hole transport materials (HTMs) for perovskite solar cells

Mohamed ADADI

## Abstract

Perovskite solar cells (PSCs) have received a lot of interest recently due to their high efficiency, affordable manufacture, and band gap tunability. Reports on PSCs efficiency rose dramatically from its initial value of 3.8% in 2009 to 24% in 2022. The absence of suitable materials for hole transportation is a significant barrier to further improving efficiency. To be used as potential components of photovoltaic systems, we have designed a series of small molecules serving as hole transport materials (HTMs) having bithiophene based donor core. The photovoltaic and optoelectronic properties of the molecules have been investigated by comparing them to a reference molecule (**R**). All the designed molecules showed lower bandgaps (1.98 eV–2.61 eV) than reference molecule (3.00 eV), indicating improved electron density transfer. All designed molecules have high open-circuit voltage (1.28 V–1.41 V) and downshifted peak occupied molecular orbital energies (- 5.41 eV to - 5.28 eV) when electron-withdrawing acceptor moieties are chosen. High dipole moments (5.18 D to 21.70 D) proved that designed molecules are highly soluble and are anticipated to make it easier to fabricate multilayered films. All designed molecules have effective charge transport capabilities, as evidenced by the reorganization energy values. All HTMs have higher FF (0.9032–0.9102) and superior power conversion efficiency of **27.40%–30.42%** compared to **R (24.62%)**. This study established the viability of fabricating high performance PSCs using all proposed molecules.

**Keywords:** TD-DFT Hole transport materials (HTM) Organic solar cells (OSCs) Perovskite solar cells (PSCs)

## Introduction

Researchers and industry have recently become engaged in perovskites solar cells (PSCs) composed of metal halide because of their interesting photophysical properties, high operational efficiency, and considerable potential in terms of low-cost assembling techniques. Researcher groups demonstrated that hole transport materials (HTMs) play a vital role in designing ideal perovskite materials. HTMs retain several unique characteristics like hole extraction and conduction, restricted charge recombination, appropriate energy levels, and long-term stability. Great advances have been made in device design and application of polymer, crosslinked, and small molecules-based HTMs over the past years. A new route for building high-performance dopant-free HTMs in PSCs has been opened by the results, which confirm the usefulness of designed strategies.

In the current study, five small donor molecules namely **TM1**, **TM2**, **TM3**, **TM4** and **TM5** have been drafted by the endcapped structural engineering of already synthesized BTT-OT-OTZDM taken as reference (**TR**).

## 1. Results and discussion

### 3.1. Geometric optimization, bond length (d) and dihedral angle ( $\theta$ )

The bond lengths (d) and the dihedral angles ( $\theta$ ) of newly designed molecules are assessed as indicated in Table 1 the order to comprehend the effects of various acceptor moieties. All newly designed molecules (**TM1-TM5**) have an average nitrogen-phenyl bond length of 1.43 Å whereas the terminal rings of sulphur and phenyl have 1.79 Å bond lengths in the reference molecule (**R**). The average bond length from donor core to bridge (**d1**) and bridge to acceptor (**d2**) was determined to be 1.46 Å and 1.43 Å. When compared to **R**, shorter bond lengths show stronger attractive forces between donor, bridge, and acceptor groups in **TM1-TM5** molecules. In **TM1-TM4** and **TM5** molecules, the dihedral angles from donor to bridge ( **$\theta_1$** ) range from -22.77281° to -20.81474° while **TM5** has 18.58855°. The dihedral angles from bridge to acceptor ( **$\theta_2$** ) in **TM1- TM5** molecules ranges from 0.69832° to 1.02775° while **TM4** molecule has 179.80218° and 13.59372° in **TM5** that increase due to reducing repulsion and penetration. The thiophene bridge has less sterically hindered than other bridges, which is related to the potential for free rotation and accounts for the variation in dihedral angle for **TM1-TM5**. It can help with the intermolecular charge transfer from donors to acceptors via the bridging fragment.

Table 1. Calculated dihedral angle and bond length between the fragments of optimized designed molecules (TM1-TM6)

Molecules	d <sub>1</sub> (Å)	d <sub>2</sub> (Å)	$\theta_1(^{\circ})$	$\theta_2(^{\circ})$
TM1	1.456	1.424	-24.983	0.839
TM2	1.455	1.420	-22.433	2.780
TM3	1.456	1.427	-23.192	1.212
TM4	1.457	1.429	-24.980	0.243
TM5	1.458	1.439	-24.601	12.888

### 3.2. Frontier molecular orbitals

The calculated HOMO and LUMO values for our reference molecule (**R**) are -5.16 eV and -1.35 eV while experimental values are -5.00 eV and -2.24 eV. HOMO values for MT1-MT6 molecules are -5.40, -5.41, -5.37, -5.28, -5.36, and -5.36 eV while LUMO values are -3.09, -3.03, -2.76, -2.85, -3.21, and -3.38 eV. The deeper HOMOs energies of MT1-MT6 molecules enhancing hole mobility, short circuit current, fill factor, and power conversion efficiency of PSCs. The band gap energies (Eg) of the studied molecules (**R**, **TM1-TM5**) are calculated using equation (3) and findings are summarized in Table 2.

$$E_g = E_{LUMO} - E_{HOMO} \quad (3)$$

Band gap energies for **R** and **TM1-TM6** molecules are calculated to be 3.81, 2.31, 2.38, 2.61, 2.43, 2.15, and 1.98 eV **TM1-TM5** molecules have lower band gap energies than reference molecule (**R**), display the effective electron transport behavior. The reference (**R**) and **TM1-TM5** molecules have band gap energies in the following order: **TM5<TM1<TM2<TM4<TM3<R**. The lower HOMO energy values of MT1-MT5 as compared to **R**, demonstrate the improved their optical and electrical characteristics. Among all, **MT4** and **MT5** molecules have lower band gap energies (2.15 eV and 1.98 eV) due to

indanand fluoro-based end capped acceptors, resulting balanced and elongated conjugation of molecules which favorable for the effective charge transporting substance.

Table 2. The calculated EHOMO (eV), ELUMO (eV), and energy band gap (Eg) of the investigated molecules (R, TM1-TM6)

Molecules	E <sub>HOMO</sub> (eV)	E <sub>LUMO</sub> (eV)	E <sub>gap</sub> (eV)
<b>R</b>	-4.969	-1.316	3.653
<b>TM1</b>	-5.227	-3.014	2.213
<b>TM2</b>	-5.160	-3.193	1.966
<b>TM3</b>	-5.213	-3.044	2.169
<b>TM4</b>	-5.093	-2.730	2.362
<b>TM5</b>	-5.093	-2.399	2.694

### 3.2. Photophysical properties

The maximum absorbance ( $\lambda_{\text{max}}$ ) of reference (R) and designed molecules (TM1-TM6) are 319, 549, 554, 522, 558, and 657 nm in the gaseous phase while 323, 601, 602, 572, 605, and 724 nm in dichloromethane solvent. The order of maximum absorbance ( $\lambda_{\text{max}}$ ) of investigated molecules in both gaseous and dichloromethane solvent is TM5>TM4> TM2>TM1>TM3>R. Among all, TM5 molecule showed a higher maximum absorbance ( $\lambda_{\text{max}}$ ) due to the presence of fluoro-based strong electron-pulling moieties and lower energy gap (1.98 eV). The newly designed molecules (TM1-TM5) have lower energy band gap (1.98 eV–2.61 eV), demonstrated a higher absorbance than the reference molecule (3.81 eV) which elevates the balanced molecular conjugation. Fig. 8 displays the normalized absorption spectra of all investigated molecules.

The excitation energies of reference and newly designed molecules (TM1-TM5) are 3.27, 2.07, 2.11, 2.33, 2.16 and 1.76 eV in the gaseous state while 3.32, 2.02, 1.96, 2.12, 1.99, and 1.66 eV in dichloromethane solvent. The comparison of the excitation energies of studied molecules (R, TM1-TM6) give the order as TM5<TM1<TM2<TM4<TM3<R for gaseous state while TM5<TM2<TM4<TM1<TM3<R for dichloromethane solvent. TM1-TM6 molecules have low energy of excitation than reference molecule which strengthened the molecule for effective charge transfer.

Table 3: The maximum absorption wavelength ( $\lambda_{\max}$ ), oscillator strength ( $f$ ), excitation energy ( $E_x$ ) and configuration interaction(%) in gaseous phase.

Molecules	$\lambda_{\max}$ (nm)	$f$	$E_x$ (ev)	Configuration (%)
<b>R</b>	389.43	1.1677	3.36	HOMO $\rightarrow$ LUMO 76
<b>DFBT1</b>	431.76	1.3352	2.99	HOMO $\rightarrow$ LUMO 44
<b>DFBT2</b>	443.98	1.7029	2.65	HOMO $\rightarrow$ LUMO 37
<b>DFBT3</b>	456.80	2.6295	2.75	HOMO $\rightarrow$ LUMO 35
<b>DFBT4</b>	463.54	2.2027	2.89	HOMO $\rightarrow$ LUMO 36
<b>DFBT5</b>	378.41	1.7206	3.12	HOMO $\rightarrow$ LUMO 38

Table 4: The maximum absorption wavelength ( $\lambda_{\max}$ ), oscillator strength ( $f$ ), excitation energy ( $E_x$ ) and configuration interaction(%) in dimethylformamide solvent.

Molecules	$\lambda_{\max}$ (nm)	$f$	$E_x$ (ev)	Configuration(%)
<b>R</b>	390.61	1.3687	3.25	HOMO $\rightarrow$ LUMO 70
<b>DFBT1</b>	444.12	1.4621	2.81	HOMO $\rightarrow$ LUMO 50
<b>DFBT2</b>	499.57	1.7658	2.48	HOMO $\rightarrow$ LUMO 39
<b>DFBT3</b>	458.49	2.4481	2.71	HOMO $\rightarrow$ LUMO 38
<b>DFBT4</b>	450.98	2.4093	2.75	HOMO $\rightarrow$ LUMO 39
<b>DFBT5</b>	396.07	1.9182	3.15	HOMO $\rightarrow$ LUMO 40

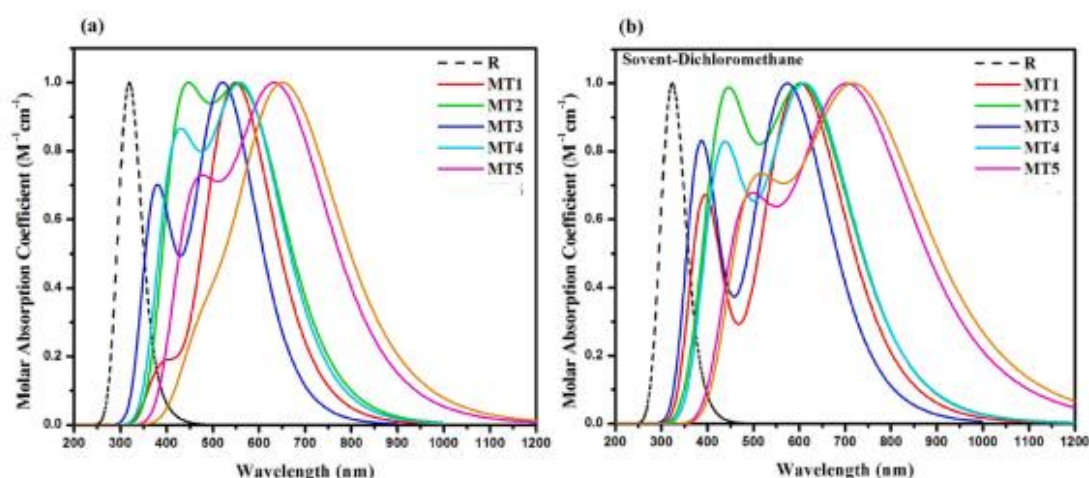


Figure 1. Normalized UV-Vis spectra of the studied molecules (R, MT1-MT6) in (a) gaseous phase and (b) solvent (dichloromethane) phase.

